Nonlinear Processes
in Geophysics

Characterization of high-intensity, long-duration continuous auroral activity (HILDCAA) events using recurrence quantification analysis

Odim Mendes[1], **Margarete Oliveira Domingues**[2], **Ezequiel Echer**[1], **Rajkumar Hajra**[3], **and Varlei Everton Menconi**[1]

[1]Space Geophysics Division (DGE/CEA), Brazilian Institute for Space Research (INPE), São José dos Campos, São Paulo, Brazil
[2]Associated Laboratory of Computation and Applied Mathematics (LAC/CTE), Brazilian Institute for Space Research (INPE), São José dos Campos, São Paulo, Brazil
[3]Laboratoire de Physique et Chimie de l'Environnement et de l'Espace (LPC2E), CNRS, Orléans 45100, France

Correspondence to: Odim Mendes (odim.mendes@inpe.br)

Abstract. Considering the magnetic reconnection and the viscous interaction as the fundamental mechanisms for transfer particles and energy into the magnetosphere, we study the dynamical characteristics of auroral electrojet (AE) index during high-intensity, long-duration continuous auroral activity (HILDCAA) events, using a long-term geomagnetic database (1975–2012), and other distinct interplanetary conditions (geomagnetically quiet intervals, co-rotating interaction regions (CIRs)/high-speed streams (HSSs) not followed by HILDCAAs, and events of AE comprised in global intense geomagnetic disturbances). It is worth noting that we also study active but non-HILDCAA intervals. Examining the geomagnetic AE index, we apply a dynamics analysis composed of the phase space, the recurrence plot (RP), and the recurrence quantification analysis (RQA) methods. As a result, the quantification finds two distinct clusterings of the dynamical behaviours occurring in the interplanetary medium: one regarding a geomagnetically quiet condition regime and the other regarding an interplanetary activity regime. Furthermore, the HILDCAAs seem unique events regarding a visible, intense manifestations of interplanetary Alfvénic waves; however, they are similar to the other kinds of conditions regarding a dynamical signature (based on RQA), because it is involved in the same complex mechanism of generating geomagnetic disturbances. Also, by characterizing the proper conditions of transitions from quiescent conditions to weaker geomagnetic disturbances inside the magnetosphere and ionosphere system, the RQA method indicates clearly the two fundamental dynamics (geomagnet-ically quiet intervals and HILDCAA events) to be evaluated with magneto-hydrodynamics simulations to understand better the critical processes related to energy and particle transfer into the magnetosphere–ionosphere system. Finally, with this work, we have also reinforced the potential applicability of the RQA method for characterizing nonlinear geomagnetic processes related to the magnetic reconnection and the viscous interaction affecting the magnetosphere.

1 Introduction

A complicated electrodynamic region populated by plasmas and ruled by the Earth's magnetic field – designated in a classical definition as magnetosphere – exists surrounding our planet (Mendes et al., 2005; Kivelson and Russell, 1995). This region is exposed to influences of the space environment and submitted to several interplanetary forcings. Initially, a summary view of the physics scenario involved is briefly described in the two following paragraphs.

In electrodynamic terms, three main solar agents ((i) electromagnetic radiation, (ii) energetic particles, and (iii) solar magnetized structures) act upon the Earth's atmosphere, which is permeated by a magnetic field created in the interior of our planet (Campbell, 2003; Hargreaves, 1992). (i) Electromagnetic radiation both heats the planet globally and ionizes the atmosphere. This ionization gives basis to a terrestrial plasma environment. (ii) Also, the incidence episodes of solar energetic particles increase the ionization in a much

more localized manner. (iii) Furthermore, escaping in a continuous way from the Sun, the solar wind, superposed sometimes by coronal mass ejection structures and other peculiar solar structures (e.g. solar fast-speed streams and heliospheric current sheet), transports intrinsically the solar magnetic field to the orbit of the Earth and beyond (Kivelson and Russell, 1995). Two primary electrodynamic interactions are possible from this incidence of the magnetized solar wind plasma upon the Earth's magnetosphere. These interactions result in a transfer of energy and particles into the magnetosphere boundary. The most intense is through the magnetic reconnection process (Burch and Drake, 2009; Kivelson and Russell, 1995; Dungey, 1961), when the interplanetary magnetic field (IMF) presenting a predominantly southward orientation, in the geocentric solar magnetosphere reference system, merges into the geomagnetic field at the outer boundary and produces strong modification in a large region formed by the magnetosphere and the ionosphere – the latter is a region from about 100 to 2000 km of altitude presenting the highest quantity of ionized particles. Another competitive process is the Kelvin–Helmholtz viscous interaction (Hasegawa et al., 1997; Chen et al., 2004; Axford and Hines, 1961). Most of the time this second process is in operation when the magnetosphere acts as a closed physical system, concerning the incident frontal solar wind, due to an IMF with northward orientation. A macroscopic fluid dynamics developed by the plasma sliding at the flanks of the magnetosphere creates a kind of viscous interaction, which produces the mixing of the solar plasma inside the magnetosphere and the occurrence of ULF waves (Menk and Waters, 2013) affecting the interior regions. The former process is more efficient in energy and particle transfer than the latter one.

In a global sense, during events of solar wind transporting IMF parallel (northward) to the frontal geomagnetic field, a regime of low magnetic disturbance on the ground is noticed. However, when the IMF is strongly southward directed, anti-parallel to the geomagnetic field, intense regimes of disturbances are recorded on the ground. Nevertheless, there is a peculiar interplanetary process related to manifestations of Alfvén waves (Guarnieri et al., 2006), presenting alternation of the magnetic component orientation (in the southward–northward direction), which produces an intermediate level of geomagnetic disturbance with the typical duration of days. These nonlinear Alfvén waves are known to be the main origin of high-intensity long-duration continuous auroral electrojet (AE) activity (HILDCAA) events on the Earth (Hajra et al., 2013; Tsurutani et al., 2011b, a; Echer et al., 2011; Tsurutani et al., 1990; Tsurutani and Gonzalez, 1987). As presented in Davis and Sugiura (1966), the AE is a geomagnetic index related to the quantification of the geomagnetic disturbance produced by enhanced ionospheric electric currents flowing below and within the auroral region (https://www.ngdc.noaa.gov/stp/geomag/ae.html). The primary mechanism for these HILDCAA events is the high-speed solar wind streams (HSSs) emanating from solar coro-

nal holes accompanied by embedded Alfvén waves (Belcher and Davis, 1971; Tsurutani et al., 1994), which are characterized by significant IMF variability (see Echer et al., 2012, 2011; Tsurutani et al., 2011b, a). The sporadic magnetic reconnection (Dungey, 1961; Gonzalez and Mozer, 1974) formed between the southward component of the Alfvén waves and the Earth's magnetopause fields leads to intense substorm/convection events comprising HILDCAAs (Tsurutani et al., 1995), which are shown to last from days to weeks (Tsurutani et al., 1995, 2006; Gonzalez et al., 2006; Guarnieri, 2006; Kozyra et al., 2006; Hajra et al., 2013, 2014a). The HILDCAA events carry a large amount of solar wind kinetic energy input into the magnetosphere affecting the polar ionosphere (Gonzalez et al., 2006; Hajra et al., 2014b). More than 60 % of this energy is dissipated in the magnetosphere–ionosphere system. Another importance of these events is the accelerated relativistic electrons, known as killer electrons, in the Earth's radiation belts (Hajra et al., 2014c, 2015b, a) for their hazardous effects on orbiting spacecraft (Wrenn, 1995; Horne, 2003). The variations of AE during HILDCAAs show the nonlinear dynamics of the physical processes involved. Therefore, a dynamical characterization is of fundamental interest for a deeper insight into the electrodynamic coupling between the solar wind and the related magnetosphere.

The aim of this work is to highlight dynamical characteristics related to the HILDCAA events revealed by the AE index in the context of the electrodynamic coupling processes. With this purpose, we apply phase space analysis, the recurrence plot (RP) technique, and the recurrence quantification analysis (RQA) method (Eckmann et al., 1987; Maizel and Lenk, 1981; Trulla et al., 1996). They constitute proper tools to treat such nonlinear, non-stationary signals as in geophysics processes. Such analysis method is applied to the HILDCAA events, for the first time to our knowledge, allowing a comparison of dynamical characteristics. By applying the nonlinear tools, this work investigates AE under some distinct physical conditions of the interplanetary medium: Alfvénic fluctuations followed by HILDCAA, Alfvénic fluctuations not followed by HILDCAA (also related to corotating interaction regions (CIRs) and high-speed streams (HSSs)), other disturbed interplanetary conditions, and geomagnetically quiet time.

This work proceeds as follows. Section 2 describes the methods for analysis. Section 3 presents the geomagnetic database and how we apply the methodology. Section 4 shows the results and interpretations. Finally, Sect. 5 summarizes the conclusions.

2   Method of analysis

Information theory structures a branch of powerful mathematical tools to analyse nonlinear systems of signal as proposed in the seminal paper of the mathematician Claude E.

Shannon (Shannon, 1964). An analogy with the concept of entropy from physics gives basis to these tools. As reviewed and discussed in detail by Cover and Thomas (2006), the entropy H used as basis for the methods can be expressed by

$$H(X) = -\sum P(x) \log(P(x)), \quad x \in X, \tag{1}$$

where X is the set of all messages $\{x_1, \ldots, x_n\}$ that X could be, and $P(x)$ is the probability of some $x \in X$. In this work, we use quantification methods associated with this theory, precisely the method developed by Zbilut and Webber Jr. (1992) of RQA that is built from the RP, as introduced in Eckmann et al. (1987), and the proprieties of the phase space, provided in the *Cross Recurrence Plot Toolbox*.[1] Initially, these methods are used to analyse dynamical systems from a theoretical point of view. Nevertheless, since the late 1990s, they have been extended to experimental data to characterize nonlinear complex behaviour (Trulla et al., 1996; Marwan and Webber, 2015). Below we summarize the phase space, the RP, and the RQA approaches.

2.1 Phase space

A phase plot is a geometric representation of the trajectories of a dynamical system in the phase plane. It is a fundamental starting point of many approaches in nonlinear data analysis, which is based on the construction of a phase space portrait of the considered system. A review of that can be found, for instance, in N. Marwan's tutorial.[2] The state of a system can be expressed by its state variables $x_1(t), x_2(t), \ldots, x_d(t)$ – for instance, the state variables density, pressure, momentum, and magnetic field for a magneto-hydrodynamics system. The d state variables at time t establish a vector in a d-dimensional space which is called phase space. The state of a system changes in time, and, consequently, the vector in the phase space describes a trajectory representing the time evolution, i.e. the dynamics of the system. Accordingly, the appearance of the trajectory retains information about the system. Therefore, the phase space is formed by coordinates that represent each significant variable of the system to specify an instantaneous state (Marwan, 2003).

In practice, observations of a real process do not unveil all state variables, or they are not known, or they cannot be measured. Nevertheless, due to the couplings between the system components, we can reconstruct a phase space trajectory from a single observation by a time delay embedding (Takens, 1981). It yields to the so-called Takens' embedding theorem, which states that a reconstruction of the phase space trajectory $\boldsymbol{x}(t)$ from a time series u_k, with a cadence Δt, allows us to present a proper dynamics of a system. In order to

do that, an embedding dimension m and a time delay τ must be identified, related to the following reconstruction:

$$\boldsymbol{x}(i) = \boldsymbol{x}_i = (u_i, u_i i + \tau, \ldots, u_{i+(m-1)\tau}), \tag{2}$$

where $t = i\Delta t$. Here, m is found by using the false nearest neighbour method and τ by the mutual information method (Kennel et al., 1992; Marwan and Webber, 2015). The idea behind this approach is to identify the influence of increasing the embedded dimension m in the number of neighbours along a trajectory of the system.

2.2 Recurrence plot

The RP is based on Poincaré's recurrence theorem from 1890, as discussed in Schulman (1978). It states that a dynamic system returns to a state arbitrarily close to the initial state after a particular time. Mathematically the RP is obtained by the square matrix

$$\mathbf{R}_{i,j} = \Theta(\epsilon_i - \| \boldsymbol{x}_i - \boldsymbol{x}_j \|), \tag{3}$$

where ϵ_i is a predefined cut-off distance, $\| . \|$ is the norm (in our case, the Euclidean norm), and $\Theta(x)$ is the Heaviside function (Eckmann et al., 1987). The binary values 0 and 1 in this matrix are represented by white and black creating visual patterns.

The characteristic typology (related to macro patterns) and texture (related to micro details) presented in the RP are the key points of the interpretation. However, the visual interpretation of RPs requires some training experience, usually done from standard systems or data libraries. For instance, as described in Marwan et al. (2007) and on the RP and RQA website http://www.recurrence-plot.tk:

i. Stationary processes are associated to homogeneous distribution of points in RP.

ii. Periodic processes present cycle patterns where the distance between periodic patterns corresponds to the period.

iii. Long diagonal lines with different distances to each other reveal a quasi-periodic process.

iv. Non-stationary processes can present interruption on the lines; they can also indicate some rare state, or RP fading to the upper left and lower right corners indicating also trend or drifts.

v. Single isolated points demonstrate heavy fluctuation in the process – in particular, if only isolated points occur, an uncorrelated or anti-correlated random process is represented.

vi. Evolutionary processes are illustrated by diagonal lines – then the evolution of states is similar at different times. However, if it has parallel lines related to the main diagonal, the system is deterministic (or even chaotic, if they

---

[1]Cross Recurrence Plot Toolbox 5.21 (R31b) by the Interdisciplinary Center for Dynamics of Complex Systems, University of Potsdam (http://tocsy.pik-potsdam.de/CRPtoolbox/).

[2]http://www.agnld.uni-potsdam.de/~marwan/matlab-tutorials/html/phasespace.html#13.

occur beside single lines), and if the diagonal lines are orthogonal to the main diagonal, or the time is reversed or the choice of embedding is insufficient.

vii. Long bowed line structures express evolution states that are similar at different epochs although they have different velocity (the dynamics of the system could be changing).

viii. Vertical and horizontal lines/clusters are evidence that a state has no or slow change for some time, which points to a laminar state.

The establishment of quantifiers to express the characterization of the processes described in RP was a significant advance in the popularization of this tool, because it can help to express in a concise and objective way a description on the dynamics of the processes, as discussed in Marwan and Webber (2015) and references therein. Therefore, quantification from RP comes primarily from the recurrence patterns, and presents for example as point density, diagonal structures, and vertical structures in the RP. In the following text, we present four of these quantifiers to study the behaviour of physical conditions such as geomagnetically quiet intervals and HILDCAA cases.

2.3 Recurrence quantification analysis

Trulla et al. (1996) addressed the problem of quantifying the structures that appear in the RPs and used them to analyse experimental data. This approach is useful to reveal qualitative transitions in a system. The corresponding measurements capture the dynamical characters of the system as represented by the signal. Therefore, RQA provides a qualitative description of a system regarding complexity measures (Marwan et al., 2007). We refer to Marwan and Kurths (2002), and Marwan (2003) for a detailed discussion on this subject. Notably, the diagonal structures in the RP and the recurrence point density are used to measure the complexity of a physical system (Zbilut and Webber Jr., 1992; Webber Jr. and Zbilut, 1994). In the present work we restrict our analysis to four characteristic parameters described below:

1. *Recurrence rate (RR)*: This denotes the overall probability that a certain state recurs and is obtained from the RP by

$$\text{RR} = \sum_{i,j=1}^{N} \frac{R_{i,j}(\rho)}{N^2}. \tag{4}$$

Larger values mean more recurrence.

2. *Determinism (DET)*: this represents how predictable a system is, and is expressed by the ratio of recurrence points that form diagonal lines of the RP of at least length $\ell_{\min}$ to all recurrence points, i.e.

$$\text{DET} = \frac{\sum_{\ell=\ell_{\min}}^{N} \ell P(\ell)}{\sum_{\ell=1}^{N} \ell P(\ell)}, \tag{5}$$

where $P(\ell)$ denotes the probability to find a diagonal line of length ℓ in the RP.

3. *Laminarity (LAM)*: this measures the occurrence of laminar states and is related to intermittent regimes – namely, it is the ratio between the recurrence points forming the vertical lines and the entire set of recurrence points computed by

$$\text{LAM} = \frac{\sum_{v=v_{\min}}^{N} v P(v)}{\sum_{v=1}^{N} v P(v)}, \tag{6}$$

where $P(v)$ denotes the probability to find a vertical line of length v in the RP. LAM does not describe the length of laminar phases. However, if this measure decreases the RP consists of more single recurrence points than vertical structures. This measurement is relatively more robust against noise in signals.

4. *Entropy (ENT)*: this reflects the complexity of the deterministic structure in the system referred to as Shannon entropy (Shannon, 1964); namely,

$$\text{ENT} = - \sum_{\ell=\ell_{\min}}^{N} p(\ell) \ln(p(\ell)), \tag{7}$$

where $p(\ell) = P(\ell)/N_\ell$. This measure reflects the complexity of the RP concerning the diagonal lines. In this form computed from RP, the interpretation of these values differ from traditional Shannon entropy – i.e. larger values are related to low entropy compared to physics analogy (Letellier, 2006).

3 Database and methodology procedure

For the present work, we have considered an updated list of 136 HILDCAA events occurring between 1975 and 2012, compiled by Hajra et al. (2013). The events were detected from the geomagnetic AE and middle- to low-latitude disturbance Dst indices by using the four strict HILDCAA criteria (Tsurutani and Gonzalez, 1987): (i) the events have peak AE intensities greater than 1000 nT, (ii) the events last for more than 2 days, (iii) high auroral activity lasts throughout the interval, i.e. AE never drops below 200 nT for more than 2 h at a time, and (iv) the events take place outside of the main phase of a geomagnetic storm. For a better understanding, the main phase is determined by the depression in the horizontal component, from middle to low latitudes, in the geomagnetic field. This behaviour is identified and quantified using the hourly value equatorial Dst index, which represents ideally the axially symmetric disturbance magnetic field at the dipole equator on the Earth's surface. This index is derived by monitoring the equatorial ring current variations (http://wdc.kugi.kyoto-u.ac.jp/dstdir/dst2/onDstindex.

Table 1. The geomagnetically quiet intervals.

Date	$K_p \leq$	AE $\leq$	Dst $\geq$
14–18 November 2000	3^0	267 nT	−20 nT
26–30 November 2001	3^-	133 nT	−50 nT
19–25 June 2004	2^0	167 nT	0 nT
19–27 June 2006	2^0	167 nT	−9 nT
15–23 July 2006	2^0	200 nT	32 nT
1–9 December 2007	3^0	200 nT	−5 nT

html). The AE data set is provided by the OMNIweb Service (http://omniweb.gsfc.nasa.gov/) by NASA and Dst from World Data Center for Geomagnetism, Kyoto Dst index service (http://wdc.kugi.kyoto-u.ac.jp/dstdir/).

From the list, the first 16 events were eliminated due to incomplete information. Among the remaining events, 33 % were preceded by geomagnetic storm main phase (Dst < −50 nT). Thus, 80 events were analysed in this work, because we selected the events classified as pure HILDCAAs, i.e. events not preceded by any geomagnetic storm main phase.

As data sets, the high-time-resolution (1 min) AE indices were analysed to study the dynamical characterization of the HILDCAA events by the RQA method. To eliminate any marginal influences, we considered a 2280 min interval centred at the middle point of a HILDCAA event. This number of records was determined by the least interval among the events.

For a quantitative comparison of disturbance geomagnetic regimes, we also performed the same RQA during the geomagnetically quiet period listed in Table 1. The quiet days follow the criteria: $K_p \leq 3^0$, Dst $\geq$ −50 nT, and AE $\leq$ 300 nT. The planetary 3 h range K_p index was introduced by J. Bartels in 1949 and designed to be sensitive to any geomagnetic disturbance affecting the Earth (http://www.gfz-potsdam.de/en/section/earths-magnetic-field/data-products-services/kp-index/explanation/). It completes a set of indices to diagnose the level of geomagnetic disturbance in a global sense. The geomagnetic indices (Rostoker, 1972) can be obtained from the World Data Center, Kyoto, at http://wdc.kugi.kyoto-u.ac.jp/wdc/Sec3.html. In that way, different physical regimes allow us to find a distinct characterization of the signals. In our case, we investigate periods of HILDCAA events that alter a physical regime that exists during the geomagnetically quiet times.

For a more complete dynamical diagnosis, this work investigates AE index under some other different physical conditions of the interplanetary medium. Completing the earlier mentioned cases of the interplanetary Alfvénic fluctuations followed by HILDCAA (related to CIRs and HSSs), and the geomagnetically quiet time, cases of interplanetary Alfvénic fluctuations not followed by HILDCAA (also related to CIRs and HSSs) and cases of intense interplanetary conditions (characterized by simultaneous activities in the AE, Dst and K_p indices) produced by different interplanetary causes are also analysed. Table 2 presents the CIRs/HSSs not followed by HILDCAA event. The first column shows the data set interval and the second column the 2280 min interval considered in the analysis calculations. Table 3 presents the events with AE index related to global intense geomagnetic disturbances. The first column shows the data set interval and the second column the 2280 min interval considered in the analysis calculations.

The analyses of the results allow a comparison of the dynamical characteristics of signals.

4 Results

Initially, two typical cases are shown and analysed, one from the HILDCAA events and another from the quiet time intervals. As examples for the methodology application, they help to understand the analysis and its interpretation. Figure 1 shows AE variations including a HILDCAA interval. The HILDCAA started at 17:34 UT on 30 May (day 150) and continued until 09:34 UT on 2 June (day 153) of 1986, with a total duration of about 64 h. In that figure, the double arrow horizontal line indicates the exact interval of the event. For the RQA calculation we consider the 2280 min interval centred at the middle of the HILDCAA. Two vertical dotted lines mark this interval. Figure 2 shows AE variations during a geomagnetically quiet period. The plot shows the geomagnetically quiet period from 17 to 22 July (day 198 to day 203) of 2006 (from Table 1). The region between the two vertical dotted lines shows the same 2280 min interval selected for the RQA study as in the HILDCAA case.

From the AE plots, the differences in the amplitudes between the HILDCAA interval (peak about 1200 nT) and the quiet time interval (peak about 300 nT) are remarkable, as expected. Both of them presents fluctuations in the signal intensities. The application of the RQA methodology aims to characterize the dynamical behaviour of the signals.
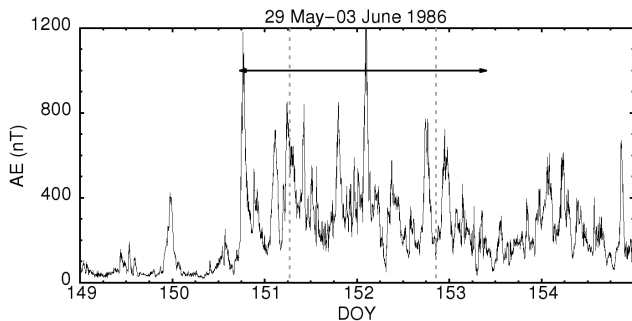
Figure 3 represents the phase space plots for the HILDCAA. As a value estimated by the earlier-mentioned mutual information methodology, the time delay (τ) used is 34 min. The phase space charts present snapshots of the interconnections of the records for each case. As described by the theory in Sect. 2, the geometric representation in the plot gives the trajectory of the dynamical system involved in the AE index records. Although slightly insinuated by the distribution of points, a proper representation is not achieved because the noise in the signal disturbs the identification of the trajectory. Following the same procedure, Fig. 4 gives the representation for the quiet interval shown earlier. The time delay (τ) found is also 34 min. Although the signal amplitude is quite different compared to the one of the HILDCAA event, the trajectory behaviour is similar. A question arises from the comparison – is it possible to distinguish from the dynami-

Table 2. CIRs/HSSs not followed by HILDCAA.

Data set interval	Interval considered
2008, 012–018 (Jan 12 to 17)	2008, Jan 14 (00:00)–15 (13:59)
2008, 030–036 (Jan 30 to Feb 4)	2008, Feb 2 (00:00)–3 (13:59)
2008, 058–064 (Feb 27 to Mar 3)	2008, Mar 2 (00:00)–3 (13:59)
2008, 165–171 (Jun 13 to 18)	2008, Jun 15 (00:00)–16 (13:59)
2008, 175–181 (Jun 23 to 28)	2008, Jun 26 (00:00)–27 (13:59)

Table 3. AE in global intense geomagnetic disturbances.

| Event	Interval considered
2012 (Mar 9)	2012, Mar 9 (00:00)–10 (13:59)
2012 (Apr 23–24)	2012, Apr 23 (00:00)–24 (13:59)
2012 (Jun 17)	2012, Jun 17 (00:00)–18 (13:59)
2012 (Jul 15)	2012, Jun 15 (00:00)–16 (13:59)

Figure 2. Geomagnetic AE index during the geomagnetically quiet period on 17 (DOY 198)–22 (203) July 2006. The AE interval used for the RQA is marked by vertical dotted lines.

Figure 1. Geomagnetic AE index from 29 May (DOY 149) to 3 June (154) 1986 includes a HILDCAA event. The HILDCAA interval is identified by the double arrow horizontal line, and the AE interval used for the RQA is shown between the vertical dotted lines.
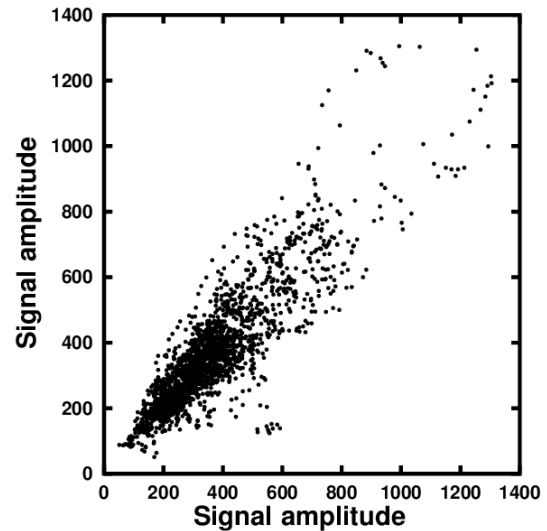
Figure 3. The phase space representation for the HILDCAA example shown in Fig. 1. The delay time is 34 min.

cal behaviour analyses the two kinds of occurrences as the AE indices point out?

To verify whether the question deserves study effort, we use the RP technique to allow a visual inspection of the signal features. Dealing with the RP theory for all the cases studied, we estimated the typical values related to these dynamical systems. The embedded dimension (m) determined by the false nearest neighbour method was found to be around 6, and following the time delay (τ) was around 34 min. The cut-off distance (ϵ) was ≈ 30 nT for the HILDCAAs, and ≈ 10 nT for the quiet intervals. For the other interplanetary conditions, the values were similar to the value of HILD-CAAs. The estimation of ϵ uses a value defined by the additive effects of the data resolution and the Gaussian noise threshold.

Related to the cases at the beginning of this section, Fig. 5 shows the RPs for the HILDCAA and Fig. 6 for the quiet interval. Here we take the embedded dimension (m) and the time delay (τ) equal to 1 for RQA calculations. These pa-

rameter choices take into account the categorization purpose of the present work, and those values do not alter our characterization process (Iwanski and Bradley, 1998; March et al., 2005; Marwan, 2011). The RPs highlight the recurrences in the signal records showing differences in the dynamical patterns between the HILDCAA interval and the quiet period. For both systems, the analyses on the large-scale patterns in the plots, designated as typology, denote that they are of the
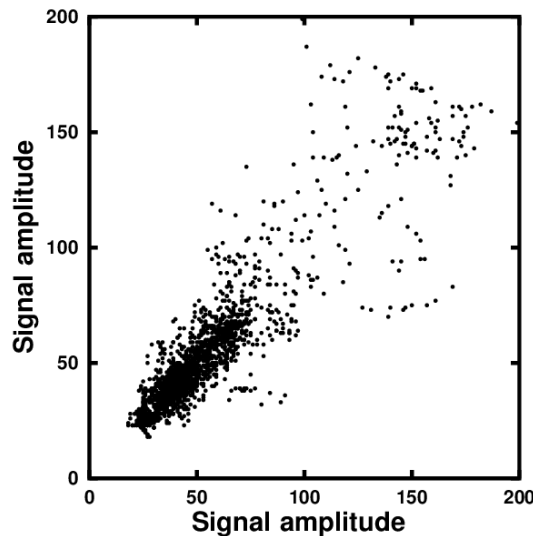
Figure 4. The phase space representation for the geomagnetically quiet period example shown, between the vertical dotted lines, in Fig. 2. The delay time is 34 min.

Table 4. RQA measures for the geomagnetically quiet interval and typical HILDCAA cases.

Case	RQA measures			
	RR	DET	LAM	ENT
Geomagnetically quiet interval	0.0203	0.357	0.518	0.719
HILDCAA period	0.0021	0.044	0.069	0.147

disrupted kind – i.e. with abrupt changes in the representation of the dynamics. However, the analysis of the small-scale patterns, designated as texture, denotes a more complex dynamics in the HILDCAA event than the one in the quiet interval. To obtain an objective interpretation, we need to translate this visual appreciation to quantitative descriptors of the dynamics of the system interpreted by the AE index. As examples of this quantification, the results of the RQA dynamical parameters for the quiet and HILDCAA case examples are presented in Table 4. We verify they are about 1 order of magnitude smaller for the HILDCAA than the values for the quiet interval. Thus, we have a little evidence that encourages this kind of study.

To pursue a comprehensive answer, we apply the RQA methodology to all 80 HILDCAA events completed by the examination of other cases selected (six geomagnetically quiet intervals, five CIRs/HSSs not followed by HILDCAA, and four events of AE in global intense geomagnetic disturbances) to allow comparisons. The values of the RQA dynamical variables (RR, DET, LAM, and ENT) were obtained for each case.

Table 5 shows the minimum, maximum, mean, standard deviation, median, and mode values estimated to the HILD-
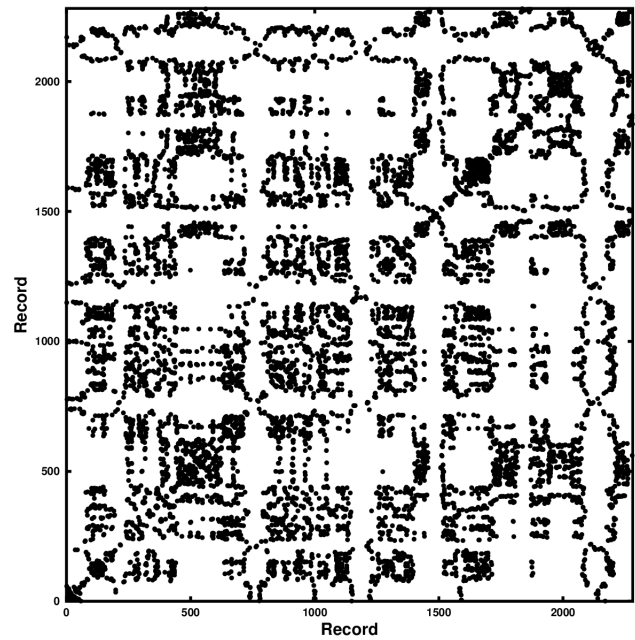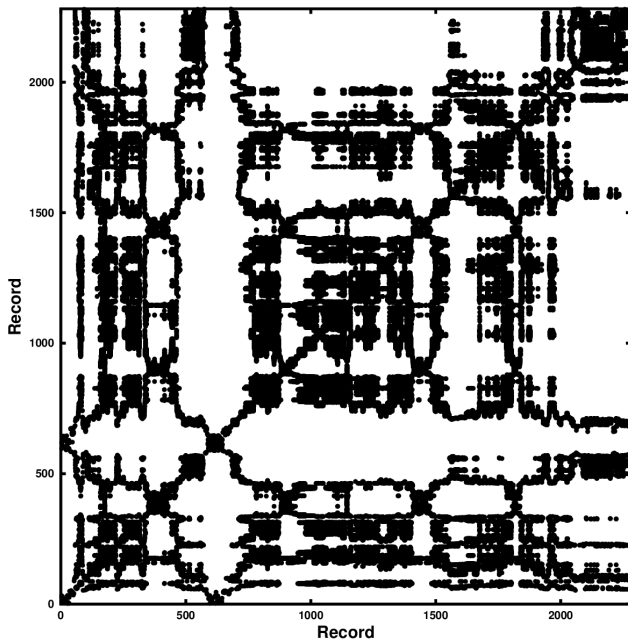

Figure 5. The RP for the HILDCAA example. The interval shown by the vertical dotted lines in Fig. 1 is used to obtain the plot.

CAAs and the quiet periods. As can be seen, a difference of 1 order of magnitude for each variable exists between these cases. For minima and maxima, the differences are between half and 1 order of magnitude. The standard deviation, median, and mode are in agreement with normal distributions for the phenomena.

Finally, Fig. 7 shows the RQA dynamical parameters for all events under study. For each parameter, we normalized the values for all events concerning extreme values obtained for the parameter. The empty circles represent the HILDCAA events, and the plus signs show the quiet periods. A clear distinction between the HILDCAA events and quiet time intervals may be noted from the figure. The separation of the results for the HILDCAA event and the quiet time interval establishes a clustering of the results, which characterize two well-defined physical regimes. Further, the symbol x indicates the results for AE index in CIR/HSS events not followed by HILDCAA, and * in a whole global disturbance scenario. As also seen in the figure, parameter behaviour is similar for CIRs/HSSs causing HILDCAAs and CIRs/HSSs not causing them, and distinct from the behaviour of quiet intervals. Therefore, based on this plot, one could say that the bottom part shows the behaviour of Alfvénic solar wind intervals, CIRs and HSSs, while the top part shows the behaviour related to the slow solar wind interval. The analysis taking into account the AE in a whole global disturbance scenario regarding geomagnetic behaviour shows larger spreading values for the parameters (except by the RR parameter); nevertheless, values are also different to the one in the quiet time regime. Based on the current geophysical knowl-

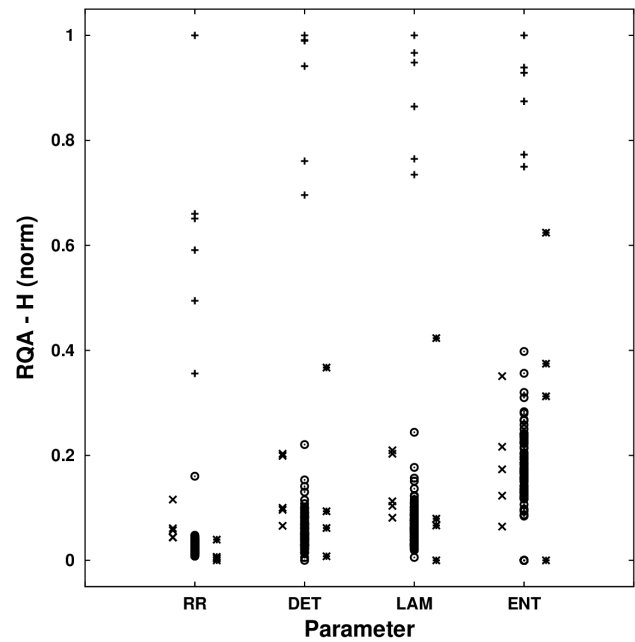**Table 5.** The RQA results considering two typical cases.

Value	HILDCAA period				Geomagnetically quiet interval			
	RR	DET	LAM	ENT	RR	DET	LAM	ENT
Min	0.0010	0.010	0.014	0.000	0.0115	0.251	0.397	0.574
Max	0.0056	0.086	0.139	0.273	0.0307	0.357	0.536	0.766
Mean	0.0016	0.031	0.049	0.091	0.0195	0.321	0.473	0.672
SD	0.0005	0.012	0.020	0.073	0.0065	0.046	0.058	0.075
Med	0.0015	0.028	0.046	0.104	0.0194	0.345	0.487	0.690
Mod	0.0013	0.010	0.014	0.000	0.0115	0.251	0.397	0.574

Figure 6. The RP for the geomagnetically quiet period example. The interval shown by the vertical dotted lines in Fig. 2 is used to obtain the plot.

Figure 7. Normalized representation of the RQA parameters for auroral electrojet (AE) indices in HILDCAA events (o), in CIRs/HSSs not followed by HILDCAA (x), in a global geomagnetic disturbance scenario (*), and in the geomagnetically quieter intervals (+).

edge, the RQA patterns in the signals for these events help to characterize/identify the standard physical features. Examining the physics of every case in the active interplanetary regimes, one might point out that the AE signature relates to HILDCAA that is connected to long-duration, large-amplitude Alfvénic fluctuations; to CIRs/HSSs not followed by HILDCAA connected to short-term Alfvénic fluctuations and with or without a small interplanetary southward magnetic amplitude; and to events in a global geomagnetic disturbance scenario connected to small-amplitude southward interplanetary magnetic field without Alfvénic fluctuations or to a large southward interplanetary magnetic amplitude.

Thus, the RQA result comparisons lead us to achieve some interpretations.

The HILDCAAs seem unique events regarding visible, intense manifestations of interplanetary Alfvénic waves; how-ever, they are similar to the other kinds of conditions regarding a dynamical signature (based on RQA), because the effect of HILDCAA is involved in the same complex mechanism of generating geomagnetic disturbances.

Allowing an interpretation of the geomagnetic disturbances, mainly the AE studied here, the physics scenario could be properly interpreted according to a basic view. As is well known, the fundamental mechanisms are the magnetic reconnection and viscous interaction with a transfer of energy and particles by electrodynamics interaction and generation of geomagnetic disturbance on ground. Supported by the parameter clustering behaviours shown in Fig. 7, the interpretation obtained from the RQA examination of AE index is in agreement with those fundamental mechanisms. Although describing an expected result, the quantitative study

using this method indicates in a clear way categories of phenomena (showed in Fig. 7). On the one hand, during geomagnetically quiet conditions, the effective interaction is the ram pressure on the solar front side of the magnetosphere and the development of viscous interaction at flanks. On the other hand, during HILDCAA events, the two fundamental electrodynamics interactions (magnetic reconnection and viscous interaction) with a transfer of energy and particles are indeed happening. In principle, interplanetary phenomena producing both of those coupling mechanisms, as processes examined in Ma et al. (2014), concern the mechanisms related to interplanetary Alfvén waves. In this kind of occurrence, magnetic disturbances can be detected by magnetometers at the polar regions as the HILDCAA events. Although they can be clearly noticed at high latitudes, those disturbances are noticed as weak worldwide manifestations. CIR/HSS occurrences not followed by HILDCAA related to short-term Alfvénic fluctuations and with or without small southward interplanetary magnetic amplitude produce sporadic, low AE index disturbances, designated as geomagnetic substorms. Events in a whole global disturbance scenario related to large southward interplanetary magnetic amplitude produce geomagnetic storms and associated geomagnetic substorms.

Identified as distinct regimes by the RQA diagnosis, the geomagnetically quiet intervals and HILDCAA events seem the proper conditions of transitions from quiescent conditions to weaker geomagnetic disturbances inside the magnetosphere and ionosphere system. Therefore, those RQA features can be useful for other study purposes. The RQA method gives a clear indication of the dynamics to be evaluated by magneto-hydrodynamics simulations, as developed by Ma et al. (2014) or Chen et al. (2004), to understand the processes involved in a transfer of energy and particles into the magnetosphere-ionosphere system.

5   Conclusions

Obtained from a diagnosis of features of a nonlinear system analysis, a physics scenario of the auroral electrojet (AE) index is built with the aid of the recurrence quantification analysis (RQA) information extracted from the recurrence plot (RP) calculation. We performed this analysis using 80 HILDCAA events completed by the examination of other cases selected (six geomagnetically quiet intervals, five CIRs/HSSs not followed by HILDCAA, and four events of AE in global intense geomagnetic disturbances) to allow comparisons.

Some significant RQA variables (RR, DET, LAM, and ENT) quantify and characterize the dynamical signatures of the AE index related to HILDCAA occurrences and other interplanetary environment conditions.

The key findings are as follows:

- The quiet intervals as compared to HILDCAA intervals are characterized by larger values of DET, LAM, and

ENT, which means higher predictability, lower entropy, and larger laminarity of the corresponding nonlinear dynamics.

- There is distinct clustering, identified by RQA, of the dynamical behaviours recorded on the ground produced by the interplanetary medium conditions: one regarding a geomagnetically quiet condition regime and another regarding an effective disturbed interplanetary regime.

- The RQA results identify similar dynamical behaviours for HILDCAA events and the other disturbed cases.

- On the one hand, the HILDCAAs seem unique events regarding the visible, intense manifestations of Alfvénic waves; on the other hand, they are similar to the other phenomena regarding dynamical signatures (based on RQA), because they are involved in the same complex mechanism of generating geomagnetic disturbances.

- This complex mechanism is composed by the magnetic reconnection and the viscous interaction implying ground geomagnetic effects triggered by the southward interplanetary magnetic field.

- One regime of clustering is AE index organized by geomagnetically quiet conditions, related to a predominant interaction from the incidence of ram pressure on the solar front side of the magnetosphere and the development of viscous interaction at flanks, while there is a northward interplanetary magnetic field (IMF). Another regime is AE organized by disturbed interplanetary conditions, with the presence of the southward IMF.

As the geomagnetically quiet intervals and HILDCAA events characterize the proper conditions of transitions from quiescent conditions to weaker geomagnetic disturbances inside the magnetosphere and ionosphere system, the RQA method gives a clear indication of the two fundamental dynamics to be evaluated with magneto-hydrodynamics simulations to understand in a better way the fundamental processes related to energy and particle transfer into the magnetosphere–ionosphere system.

With the present work, we have also demonstrated the potential applicability of the RQA method for characterizing of nonlinear geomagnetic processes related to magnetic reconnection and viscous interaction affecting the magnetosphere, mainly with the aid of magneto-hydrodynamics simulations.

References

Axford, W. I. and Hines, C. O.: A unifying theory of high-latitude geophysical phenomena and geomagnetic storms, C. J. Phys., 39, 1433–1464, https://doi.org/10.1139/p61-172, 1961.

Belcher, J. W. and Davis, L. J.: Large-amplitude Alfvèn waves in the interplanetary medium: 2, J. Geophys. Res., 76, 3534–3563, 1971.

Burch, J. L. and Drake, J. F.: Reconnecting magnetic fields, Am. Sci., 97, 392–399, 2009.

Campbell, W. H.: Introduction to geomagnetic fields, Cambridge, 2003.

Chen, Q., Otto, A., and Lee, L. C.: Tearing instability, Kelvin-Helmholtz instability, and magnetic reconnection, J. Geophys. Res., 430, 1755–1758, 2004.

Cover, T. M. and Thomas, J. A.: Elements of Information Theory, Wiley-Interscience, New Jersey, 2006.

Davis, T. N. and Sugiura, M.: Auroral electroject activity index AE and its universal time variations, J. Geophys. Res,, 71, 785, https://doi.org/10.1029/JZ071i003p00785, 1966.

Dungey, J. W.: Interplanetary magnetic field and the auroral zones, Phys. Rev. Lett., 6, 47–48, 1961.

Echer, E., Gonzalez, W. D., Tsurutani, B. T., and Kozyra, J. U.: High speed stream properties and related geomagnetic activity during the whole heliospheric interval, Sol. Phys., 274, 303–320, https://doi.org/10.1007/s11207-011-9739-0, 2011.

Echer, E., Tsurutani, B. T., and Gonzalez, W. D.: Extremely low geomagnetic activity during the recent deep solar cycle minimum, Proc. Int. Astron. Union, 7, 200–209, https://doi.org/10.1017/S174392131200484X, 2012.

Eckmann, J. P., Kamphorst, S., and Ruelle, D.: Recurrence plots of dynamical systems, Europhys. Lett., 4, 973–977, 1987.

Gonzalez, W. D. and Mozer, F. S.: A quantitative model for the potential resulting from reconnection with an arbitrary interplanetary magnetic field, J. Geophys. Res., 79, 4186–4194, 1974.

Gonzalez, W. D., Guarnieri, F. L., Clua-Gonzalez, A. L., Echer, E., Alves, M. V., Oginoo, T., and Tsurutani, B. T.: Recurrent Magnetic Storms: Corotating Solar Wind Streams, chap. Magnetospheric energetics during HILDCAAs, AGU, https://doi.org/10.1029/167GM15, 2006.

Guarnieri, F. L.: Recurrent Magnetic Storms: Corotating Solar Wind Streams, chap. The nature of auroras during high-intensity long-duration continuous AE activity (HILDCAA) events: 1998–2001, AGU, https://doi.org/10.1029/167GM19, 2006.

Guarnieri, F. L., Tsurutani, B. T., Gonzalez, W. D., Clua-Gonzalez, A. L., Grande, M., Soraas, F., and Echer, E.: ICME and CIR storms with particular emphases on HILDCAA events, in: ILWS WORKSHOP 2006, COSPAR, GOA, India, 2006.

Hajra, R., Echer, E., Tsurutani, B. T., and Gonzalez, W. D.: Solar cycle dependence of high-intensity long-duration continuous AE activity (HILDCAA) events, relativistic electron predictors?, J. Geophys. Res., 118, 5626–5638, https://doi.org/10.1002/jgra.50530, 2013.

Hajra, R., Echer, E., Tsurutani, B. T., and Gonzalez, W. D.: Superposed epoch analyses of HILDCAAs and their interplanetary drivers: solar cycle and seasonal dependences, J. Atmos. Sol. Terr. Phys., 121, 24–31, https://doi.org/10.1016/j.jastp.2014.09.012, 2014a.

Hajra, R., Echer, E., Tsurutani, B. T., and Gonzalez, W. D.: Solar wind-magnetosphere energy coupling efficiency and partitioning: HILDCAAs and preceding CIR storms during solar cycle 23,, J. Geophys. Res., 119, 2675–2690, https://doi.org/10.1002/2013JA019646, 2014b.

Hajra, R., Tsurutani, B. T., Echer, E., and Gonzalez, W. D.: Relativistic electron acceleration during high-intensity, long-duration, continuous AE activity (HILDCAA) events: solar cycle phase dependences, Geophys. Res. Lett., 41, 1876–1881, https://doi.org/10.1002/2014GL059383, 2014c.

Hajra, R., Tsurutani, B. T., Echer, E., Gonzalez, W. D., Brum, C. G., Vieira, L. E. A., and Santolik, O.: Relativistic electron acceleration during HILDCAA events: are precursor CIR magnetic storms important?, Earth, Planets Space., 67, https://doi.org/10.1186/s40623-015-0280-5, 2015a.

Hajra, R., Tsurutani, B. T., Echer, E., Gonzalez, W. D., and Santolik, O.: Relativistic (E > 0.6, > 2.0, and > 4.0 mev) electron acceleration at geosynchronous orbit during high-intensity, long-duration, continuous AE activity (HILDCAA) events, Astrophys. J., 799, https://doi.org/10.1088/0004-637X/799/1/39, 2015b.

Hargreaves, J. K.: The solar-terrestrial environment, Camnbridge, 1992.

Hasegawa, H., Fujimoto, M., Phan, T. D., Rème, H., Balogh, A., Dunlop, M. W., Hashimoto, C., and TanDokoro, R.: Transport of solar wind into Earth's magnetosphere through rolled-up Kelvin-Helmholtz vortices, Nature, 102, 151–161, 1997.

Horne, R. B.: Rationale and requirements for a european space weather programme, in: Space Weather Workshop: Looking Towards a European Space Weather Programme, pp. 139–144, European Space Agency, Nordwijk, the Netherlands, 2003.

Iwanski, J. S. and Bradley, E.: Recurrence plots of experimental data: to embedded or not to embed?, Chaos, 8, 861–871, 1998.

Kennel, M. B., Brown, R., and Abarbanel, H. D. I.: Determining embedding dimension for phase-space reconstruction using a geometrical construction, Phys. Rev. A, 45, 3403, https://doi.org/10.1103/PhysRevA.45.3403, 1992.

Kivelson, M. G. and Russell, C. T. (Eds.): Introduction to Space Physics, Cambridge, 2 edn., 1995.

Kozyra, J. U., Crowley, G., Emery, B. A., Fang, X., Maris, G., Mlynczak, M. G., Niciejewski, R. J., Palo, S. E., Paxton, L. J., Randall, C. E., Rong, P. P., Russell, J. M., Skinner, W., Solomon, S. C., Talaat, E., Wu, Q., and Yee, J. H.: Recurrent Magnetic Storms: Corotating Solar Wind Streams, chap. Response of the upper/middle atmosphere to coronal holes and powerful high-speed solar wind streams in 2003, AGU, https://doi.org/10.1029/167GM24, 2006.

Letellier, C.: Estimating the Shannon Entropy: Recurrence Plots versus Symbolic Dynamics, Phys. Rev. Lett., 96, 254102-1–254102-4, 2006.

Ma, X., Otto, A., and Delamere, P. A.: Interaction of magnetic reconnection and kelvin-helmholtz modes for large magnetic shear: 1. kelvin-helmholtz trigger, J. Geophys. Res.-Space Physics, 119, 781–797, https://doi.org/10.1002/2013JA019224, 2014.

Maizel, J. V. and Lenk, R. P.: Enhanced graphic matrix analysys of nucleic acid and protein sequences, Genetic, P. Natl. Acad. Sci. USA, 78, 7665–7669, 1981.

March, T. K., Chapman, S. C., and Dendy, R. O.: Recurrence plot statistics and the effect of embedding, Phys. D, 200, 173–184, 2005.

Marwan, N.: Encounters with neighbours. current developments of concepts based on recurrence plots and their applications, Ph.D. thesis, Institut Für Physik, Fakultät Mathematik und Naturwissenschaften, Universität Potsdam, 2003.

Marwan, N.: How to avoid potential pitfalls in recurrence plot based data analysis, Int. J. Bifurcation Chaos, 21, 1003, 2011.

Marwan, N. and Kurths, J.: Nonlinear analysis of bivariate data with cross recurrence plots, Phys. Lett. A, 302, 299–307, https://doi.org/10.1016/S0375-9601(02)01170-2, 2002.

Marwan, N. and Webber, C. L. J.: Recurrence Quantification Analysis, chap. Mathematical and computational foundations of recurrence quantifications, 3–43, Springer, 2015.

Marwan, N., Carmen, M., Romano, M. T., and Kurths, J.: Recurrence plots for the analysis of complex systems, Phys. Reports, 438, 237–329, https://doi.org/10.1016/j.physrep.2006.11.001, 2007.

Mendes, O., Domingues, M. O., and da Costa, A. M.: Introduction to planetary electrodynamics: a view of electric fields, currents and related magnetic fields, Adv. Space Res., 35, 812–828, https://doi.org/10.1016/j.asr.2005.03.139, 2005.

Menk, F. and Waters, C. L.: Magnetoseismology, Wiley-VCH, 1 edn., 2013.

Rostoker, G.: Geomagnetic indices, Rev. Geophysics, 10, 935–950, https://doi.org/10.1029/RG010i004p00935, 1972.

Schulman, L. S.: Note on the quantum recurrence theorem, Phys. Rev. A, 18, 2379–2380, 1978.

Shannon, C. E.: The Mathematical Theory of Communication, University of Illinois, Urbana, IL, University of Illinois, Urbana, IL, 1964.

Takens, F.: Dynamical Systems and Turbulence, Warwick 1980, vol. 898, chap. Detecting strange attractors in turbulence, 366–381, Springer Berlin Heidelberg, Berlin, https://doi.org/10.1007/BFb0091924, 1981.

Trulla, L. L., Giuliani, A., Zbilut, J. P., and Webber, C. L. J.: Recurrence quantification analysis of the logistic equation with transients, Phys. Lett. A, 223, 255–260, 1996.

Tsurutani, B. T. and Gonzalez, W. D.: The cause of High-Intensity, Long-Duration, Continuous AE Activity (HILDCAAs): interplanetary Alfvèn wave trains, Planet. Space Sci., 35, 405, 1987.

Tsurutani, B. T., Gould, T., Goldstein, B. E., Gonzalez, W. D., and Sugiura, M.: Interplanetary Alfvèn waves and auroral (substorm) activity: IMP 8, J. Geophys. Res., 95, 2241–2252, https://doi.org/10.1029/JA095iA03p02241, 1990.

Tsurutani, B. T., Ho, C., Smith, E. J., Neugebauer, M., Goldstein, B. E., Mok, J. S., Arballo, J. K., Balogh, A., Southwood, D. J., and Feldman, W. C.: The relationship between interplanetary discontinuities and Alfvèn waves: Ulysses observations, Geophys. Res. Lett., 21, 2267–2270, https://doi.org/10.1029/94GL02194, 1994.

Tsurutani, B. T., Gonzalez, W. D., Clua-Gonzalez, A. L., Tang, F., Arballo, J. K., and Okada, M.: Interplanetary origin of geomagnetic activity in the declining phase of the solar cycle, J. Geophys. Res., 100, 21717–21733, 1995.

Tsurutani, B. T., Gonzalez, W. D., lua-Gonzalez, A. L., Guarnieri, F. L., Gopalswamy, N., Grande, M., Kamide, Y., Kasahara, Y., Mann, I., Lu, G., McPherron, R., Soraas, F., and Vasyliunas, V.: Corotating solar wind streams and recurrent geomagnetic activity: a review, J. Geophys. Res., 111, A07S01, https://doi.org/10.1029/2005JA011273, 2006.

Tsurutani, B. T., Echer, E., and Gonzalez, W. D.: The solar and interplanetary causes of the recent minimum in geomagnetic activity (MGA23): a combination of midlatitude small coronal holes, low IMF B_Z variances, low solar wind speeds and low solar magnetic fields, Ann. Geophys., 29, 839–849, https://doi.org/10.5194/angeo-29-839-2011, 2011a.

Tsurutani, B. T., Echer, E., Guarnieri, F. L., and Gonzalez, W. D.: The properties of two solar wind high speed streams and related geomagnetic activity during the declining phase of solar cycle 23, J. Atmos. Sol. Terr. Phys., 73, 164–177, 2011b.

Webber Jr., C. L. and Zbilut, J. P.: Dynamical assessment of physiological systems and states using recurrence plot strategies, J. Appl. Physiol., 76, 965–973, 1994.

Wrenn, G. L.: Conclusive evidence for internal dielectric charging anomalies on geosynchronous communications spacecraft, J. Spacecraft Rockets, 32, 514–520, 1995.

Zbilut, J. P. and Webber Jr., C. L.: Embeddings and delays as derived from quantification of recurrence plots, Phys. Lett. A, 171, 199–203, 1992.